0026-895X/92/020412-07$03.00/0
Copyright © by The American Society for Pharmacology and Experimental Therapeutics
All rights of reproduction in any form reserved.
MOLECULAR PHARMACOLOGY, 41:412-418

MOL PHARM

Interaction of Tetrahydroaminoacridine with Acetylcholinesterase and Butyrylcholinesterase

HARVEY ALAN BERMAN and KATHRYN LEONARD

Department of Biochemical Pharmacology, State University of New York at Buffalo, Buffalo, New York 14260

Received June 7, 1991; Accepted October 31, 1991

SUMMARY

This paper examines inhibition of acetylcholinesterase (AchE) and butyrylcholinesterase (BuchE) by tetrahydroaminoacridine (THA), an acridine analog under consideration for palliative treatment of Alzheimer's dementia. THA causes linear mixed inhibition of AchE hydrolysis of acetylthiocholine, a cationic substrate (K_I = 3.8 × 10^{-9} M), and linear competitive inhibition of AchE hydrolysis of 7-acetoxy-4-methylcoumarin, an uncharged substrate (K_I = 6.8 × 10^{-9} M), and *N*-methyl-7-dimethylcarbamoxyquinolinium, a cationic carbamate (K_I = 1.5 × 10^{-8} M). Propidium association with AchE in the presence of saturating concentrations of THA is characterized by a dissociation constant of 7.7 ± 0.7 × 10^{-6} M, a value within 2-fold of the dissociation constant in the absence of THA. Association of THA with AchE is, therefore, not mutually exclusive with association of propidium at the peripheral anionic site. Moreover, THA causes dissociation of decidium complexes with AchE at concentrations compatible with a dissociation constant of 7.0 ± 0.4 × 10^{-9} M. Similar relationships were observed for THA inhibition of BuchE hydrolysis of butyrylthiocholine (K_I = 2.5 × 10^{-8} M) and dissociation of decidium complexes with BuchE (K_D = 1.9 ± 0.1 × 10^{-8} M). These kinetic and equilibrium data uniformly indicate that THA associates with AchE and BuchE with high affinity and that the subsequent inhibition comes about through ligand association at the active center rather than at a peripheral site. The noncompetitive component of inhibition reflects association of THA with the acyl-enzyme intermediate, with subsequent effects on the rate of deacylation.

Alzheimer's dementia is a progressive neurodegenerative disorder characterized as a loss of short and long term memory, cognitive function, and intellectual facility (1, 2). Examination of cortical and hippocampal brain sections from Alzheimer's patients reveals the presence of neuritic plaques and neurofibrillary tangles, abnormal structures that have come to represent hallmarks of this disorder. Alzheimer's disease occurs also with a progressive loss from the cortex and hippocampus of cholinergic neurons, with accompanying reductions in the numbers of muscarinic receptors, choline acetyltransferase, Ach^+, and AchE (3–5).

The pronounced alteration in proteins associated with cholinergic neurotransmission has provided a pharmacologic rationale for palliative treatment of this disorder. In particular, the reduced muscarinic receptor density and amounts of Ach^+ have prompted investigation of a number of potential inhibitors of AchE (6). One of the principal drugs under current investigation for use in the treatment of Alzheimer's disease is THA, known also as tacrine (Ref. 7, but see Refs. 8 and 9). Although THA has long been known to cause inhibition of AchE and BuchE (10, 11), the molecular mechanism and site specificity underlying inhibition remain unknown.

This paper uses kinetic and equilibrium techniques to examine THA inhibition of AchE from *Torpedo californica* and the topographic specificity underlying inhibition. The kinetics of noncovalent reversible inhibition are examined with respect to three kinetically distinct synthetic substrates for which the relative rates of acylation and deacylation differ. The three substrates are $AcSch^+$, a cationic acetate, 7AMC, an uncharged acetate, and M7C, a cationic carbamate. Topographic specificity is assessed with respect to ligand association at the active center and the peripheral anionic site, a distinct anionic locus spatially removed from the active center. The fluorescent ligand propidium is used as a selective probe for the peripheral anionic site (12). Active center occupation is assessed through competitive interactions with decidium, a fluorescent ligand that binds with its trimethylammonium moiety within the active center (13–15). Results for AchE are compared with those obtained for an homologous enzyme, BuchE, from human plasma.

This work was supported by grants from the National Institutes of Health (ES-03085) and the United States Army Research Office, Research Triangle Park, NC.

[1]H. A. Berman and K. J. Leonard, unpublished results.

ABBREVIATIONS: Ach^+, acetylcholine; AchE, acetylcholinesterase; BuchE, butyrylcholinesterase; $AcSch^+$, acetylthiocholine; 7AMC, 7-acetoxy-4-methylcoumarin; 7HMC, 7-hydroxy-4-methylcoumarin; $BuSch^+$, butyrylthiocholine; NMA, *N*-methylacridinium; M7C, *N*-methyl-7-dimethylcarbmoxyquinolinium; THA, tetrahydroaminoacridine.

MOLECULAR PHARMACOLOGY
aspet
Downloaded from molpharm.aspetjournals.org at Universidade do Estado do Rio de Janeiro on December 4, 2012

Experimental Procedures

Materials. AchE from *T. californica* was isolated by affinity chromatography as described by Taylor *et al.* (16). In all experiments reported, the enzyme specific activity was in the range of 5–7 μmol of Ach^+ hydrolyzed/min/μg of protein. BuchE from human plasma was isolated to homogeneity by procedures described by Lockridge and La Du (17) and Ralston *et al.* (18). In addition, as a first step, fresh unfrozen plasma was stirred at 4° for at least 24 hr in the presence of $CaCl_2$ (20 mM) and then filtered through cheesecloth; this procedure served to remove clotting proteins and to facilitate subsequent ion exchange and affinity chromatography procedures. As a final step, after elution of the enzyme from a DEAE-Sephadex A-50 column with a linear choline chloride gradient, the fractions containing BuchE were pooled, dialyzed against a 50 mM sodium phosphate buffer, pH 8.0, containing 0.1 N NaCl, and passed through a Sephadex G-200 column to afford electrophoretically pure enzyme; this gel filtration procedure served to remove low molecular weight contaminants that were evident on sodium dodecyl sulfate-polyacrylamide gel electrophoresis. In all experiments, the enzyme specific activity was in the range of 400–800 μmol of $BuSch^+$/min/mg. Decidium diiodide and 7AMC were prepared as already described (15, 19). Propidium diiodide, NMA, 7HMC, and M7C iodide were obtained from Molecular Probes (Eugene, OR). $AcSch^+$ iodide, $BuSch^+$ chloride, and THA were obtained from Sigma Chemical Co. (St. Louis, MO). Kinetic determinations of $AcSch^+$ and 7AMC hydrolysis were carried out at 23° in 0.01 M sodium phosphate, pH 7.0, containing 0.2 M NaCl. Kinetic determination of M7C hydrolysis and all equilibrium fluorescence titrations were carried out at 23° in a 0.01 M Tris·HCl buffer, pH 8.0, containing 0.1 M NaCl and 0.04 M $MgCl_2$.

Fluorescence titrations and spectral determinations were carried out on SPEX 212 and Aminco-Bowman spectrofluorimeters. Changes in absorbance were recorded on a Perkin-Elmer Lambda 3B spectrophotometer connected through a Data Translation 2805 analog-to-digital converter resident in an IBM PC computer; data acquisition was controlled with Lab Tech Notebook (Laboratory Technologies, Cambridge, MA).

Kinetics of reversible inhibition. Enzymatic hydrolysis of $AcSch^+$ in the presence of 5,5′-dithio-bis(2-nitrobenzoic acid) (3.3×10^{-4} M) and the presence or absence of cationic ligands was measured by monitoring absorbance at 412 nm as a function of time (20). These procedures have already been described with respect to catalysis by AchE (19). For BuchE, enzyme activity was measured in a similar manner with respect to hydrolysis of $BuSch^+$. For each determination, spontaneous breakdown of substrate was accounted for in a reference cuvette containing all materials except enzyme. Reaction velocities were calculated as the change in absorbance per unit time. Liberation of thiocholine was quantitated using an extinction coefficient for the thionitrobenzoate dianion of 14,150 M^{-1} cm^{-1} (21). Enzymatic hydrolysis of 7AMC was measured by monitoring fluorescence of the product 7HMC at 450 nm, upon excitation at 360 nm, as described by Berman and Leonard (19). Enzymatic hydrolysis of M7C was measured by monitoring fluorescence of the product *N*-methyl-7-hydroxyquinolinium at 500 nm, upon excitation at 400 nm, as described previously (15); in this case, hydrolysis rate constants (sec^{-1}) were obtained by analysis of the exponential burst remaining after stripping of the slow linear component representative of decarbamylation.

Equilibrium fluorescence titrations. Equilibrium titrations of AchE with propidium and decidium were conducted by monitoring ligand fluorescence at 610 nm, upon excitation at 535 nm. For titration of BuchE, ligand fluorescence was monitored at 590 nm, upon excitation at 535 nm. Data acquisition and analysis have already been described (13–15).

The dissociation constant for THA was determined from its capacity to cause dissociation of decidium complexes with AchE or BuchE. In these experiments, decidium was present at concentrations >20 times its respective dissociation constant and in a stoichiometry at least 2 times the enzyme normality; these conditions obviate consideration of uncomplexed sites. The observed fluorescence intensity of decidium, f, was related to the free concentration of decidium, $[F]$, and competing nonfluorescent ligand, $[C]$, according to the following equation,

$$(f_F - f)/(f - F_C) = (K_F/K_C)\ [C]/[F]$$

where f_F and f_C denote, respectively, the initial fluorescence when all sites are complexed with decidium and the final fluorescence when all sites are complexed with competing ligand. K_F and K_C denote the respective dissociation constants for decidium and competing ligands. A logarithmic plot of $f_F - f/f - f_C$ versus $[C]/[F]$ gives a slope of unity for competitive dissociation at a homogeneous class of independent sites. The x-axis represents the ratio of the free concentrations of the competitive nonfluorescent (C) and fluorescent (F) ligands.

Noncovalent inhibition of AchE. A general form for equilibrium reversible inhibition is described by scheme I, where E, S, and ES denote free enzyme, free substrate, and enzyme-substrate complex, respectively. ES undergoes covalent reaction to regenerate free enzyme and product, P. In the presence of inhibitor, I, two noncovalent complexes can form, the enzyme-inhibitor complex EI and a ternary complex, ESI, containing enzyme, substrate, and inhibitor. K_S and K_I refer, respectively, to the substrate and inhibitor dissociation constants. This scheme ignores formation of any covalent intermediates that occur after formation of ES and ESI but before production of P.

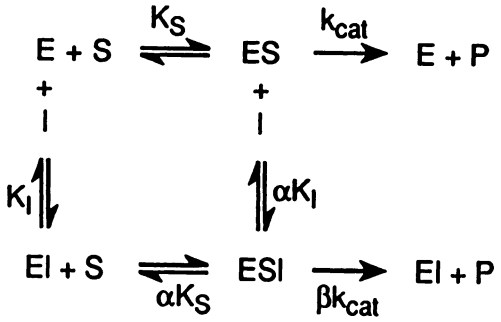

SCHEME I

The reciprocal form of the velocity equation for enzyme inhibition that satisfies scheme I is given in eq. 1, where $[E_O]$ refers to the initial enzyme concentration, and $V_{max} = k_{cat}[E_O]$.

$$1/V = (K_S/V_{max})\{(1 + ([I]/K_I))/(1 + (\beta[I]/\alpha K_I))\}(1/[S]) + 1/V_{max}\{(1 + ([I]/\alpha K_I))/(1 + (\beta[I]/\alpha K_I))\} \quad (1)$$

When $\beta = 0$, ESI is nonproductive and linear inhibition is obtained. Replots of slope versus $[I]$ are linear and intersect the $[I]$ axis at a value equal to $-K_I$. Values of $\alpha \gg 1$ indicate that formation of the ternary complex ESI is negligible, and scheme I reduces to competitive inhibition. In pure noncompetitive ($\alpha = 1$) and mixed inhibition ($\alpha > 1$), the y-intercept versus $[I]$ replots are linear but intersect the $[I]$ axis at a value equal to $-\alpha K_I$.

Results

Reversible noncovalent inhibition of AchE hydrolysis and BuchE hydrolysis. THA displayed linear mixed inhibition of AchE hydrolysis of $AcSch^+$ (Fig. 1). This behavior was indicated by intersection of the double-reciprocal lines in the upper left quadrant and the linear slope versus $[I]$ replot. From the x-intercept of the slope replot, the inhibition constant K_I was determined to be 3.8×10^{-9} M. The y-intercept replot was linear and afforded a value for α of 1.5. On the basis of scheme I, the low value of α indicated that THA showed comparable affinity for both free enzyme and the enzyme-substrate complex, and this was indicative of a strongly noncompetitive mode of reversible inhibition. The inhibition constant obtained here

MOL PHARM
MOLECULAR PHARMACOLOGY
aspet
Downloaded from molpharm.aspetjournals.org at Universidade do Estado do Rio de Janeiro on December 4, 2012

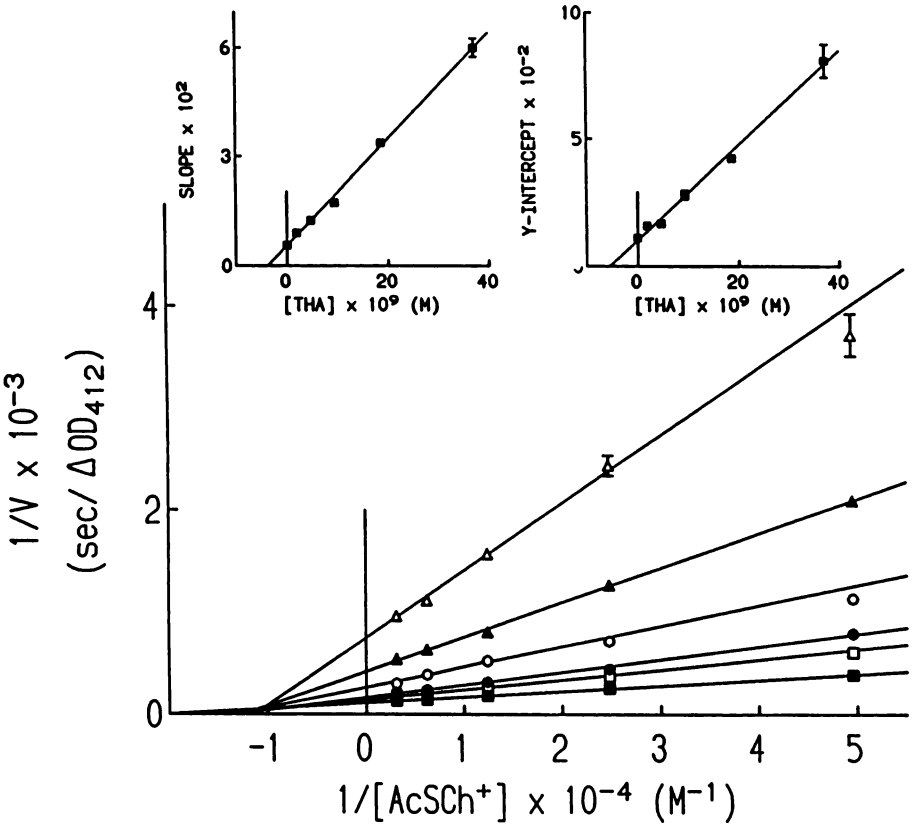

Fig. 1. Double-reciprocal plots for inhibition by THA of AchE hydrolysis of $AcSch^+$. The enzyme was present at a concentration of 1.7×10^{-10} M, in a reaction medium of 0.01 M sodium phosphate buffer, pH 7.0, containing 0.2 M NaCl. ■, No THA; □, 1.88 nM; ●, 4.69 nM; ○, 9.36 nM; ▲, 18.7 nM; △, 37.2 nM. The value for k_{cat}, taken from the reciprocal of the *y*-intercept, was calculated to be 2.2×10^5 min^{-1}. The value for K_S, taken from the reciprocal of the *x*-intercept, was calculated to be 5.0×10^{-5} M. *Upper left inset*, replot of the reciprocal plot slopes versus THA concentration; the inhibition constant taken from the [*I*]-intercept was calculated to be 3.8×10^{-9} M. *Upper right inset*, *y*-intercept replot, from which α was determined to be 1.5. The data are indicative of linear mixed inhibition.

is compatible with the value of 8.5×10^{-9} M for the noncompetitive inhibition constant obtained for *Torpedo* AchE by Wu and Yang (22) but is much lower than the value of 2.2×10^{-6} M obtained by Patocka *et al.* (11) for human erythrocyte AchE.

THA displayed linear competitive inhibition of 7AMC hydrolysis by AchE (Fig. 2). In this case, slopes of the double-reciprocal plots increased in a linear manner with increasing THA concentration, without alteration in the *y*-intercept. The value of K_I estimated from the slope replot was 6.8×10^{-9} M, in close agreement with that obtained with $AcSch^+$ as substrate.

THA displayed linear competitive inhibition of M7C hydrolysis (Fig. 3). M7C is of interest because it forms a long-lived carbamyl-enzyme intermediate, thereby enabling examination of the acyl-transfer step without consideration of the kinetic parameters associated with deacylation of the complex. In this case, the competitive inhibition constant, estimated from the slope replot, was 1.5×10^{-8} M, within 2–3-fold of the values observed for $AcSch^+$ and 7AMC.

Linear mixed inhibition was observed for interaction of THA with BuchE (Fig. 4). From the *x*-intercept of the slope replot, the value of K_I was determined to be 2.5×10^{-8} M. The *y*-intercept replot was linear and afforded a value for α of 1.7.

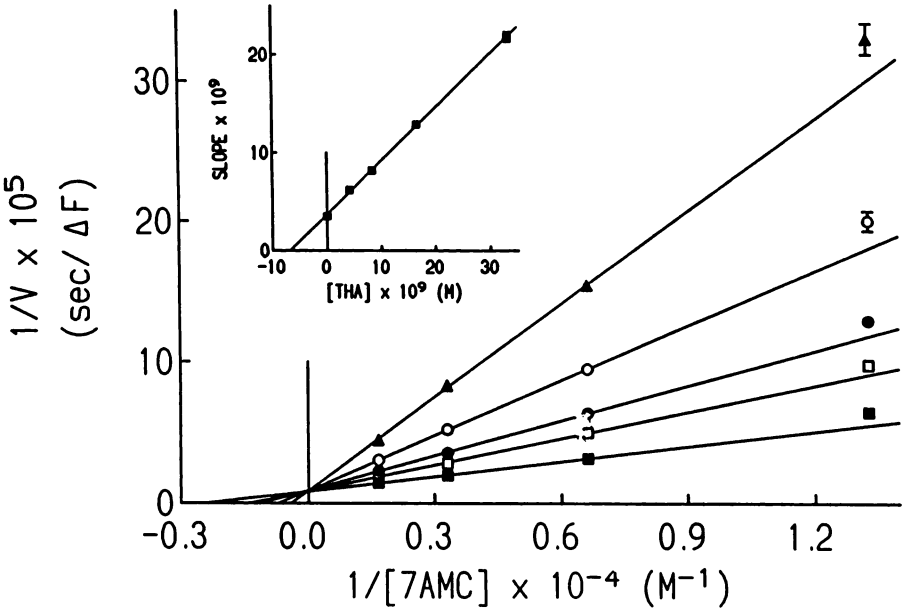

Fig. 2. Double-reciprocal plots for inhibition by THA of AchE hydrolysis of 7AMC. The enzyme was present at a concentration of 2.0×10^{-9} M, in a reaction medium of 0.01 M sodium phosphate buffer, pH 7.0, containing 0.2 M NaCl. ■, No THA; □, 4.16 nM; ●, 8.32 nM; ○, 16.6 nM; ▲, 33.3 nM. The value for k_{cat} was calculated to be 7.4×10^3 min^{-1}. For this calculation, the number of equivalents of 7HMC liberated upon hydrolysis was obtained by comparing the fluorescence value from the reciprocal of the *y*-intercept with the intensities of known concentrations of 7HMC. The value for K_S was 4.2×10^{-4} M. *Inset*, replot of the reciprocal plot slopes versus THA concentration. The [*I*]-intercept of the replot affords a competitive inhibition constant of 6.8×10^{-9} M. The data are indicative of linear competitive inhibition.

MOL PHARM
MOLECULAR PHARMACOLOGY
aspet
Downloaded from molpharm.aspetjournals.org at Universidade do Estado do Rio de Janeiro on December 4, 2012

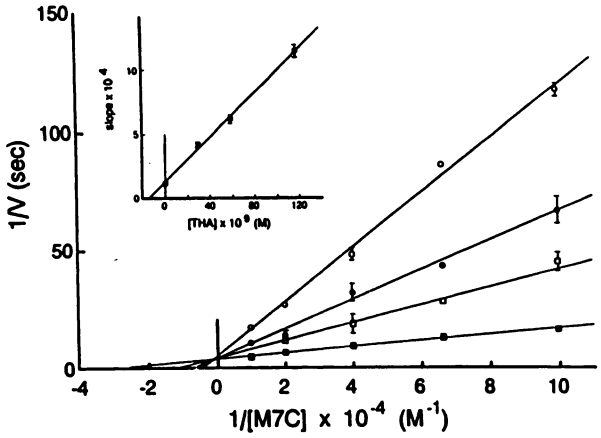

Fig. 3. Double-reciprocal plots for inhibition by THA of AchE hydrolysis of M7C. The enzyme was present at a concentration of 1.5×10^{-8} M, in a reaction medium of 0.01 M Tris·HCl, pH 8.0, containing 0.1 M NaCl and 0.04 M $MgCl_2$. ■, No THA; □, 29.7 nM; ●, 59.3 nM; ○, 118 nM. The value for k_2, the rate constant for carbamylation, was calculated from the reciprocal of the y-intercept to be 0.25 sec^{-1}. The value for K_S was 30.5×10^{-6} M. *Inset*, replot of the reciprocal plot slopes versus THA concentration. The [*I*]-intercept of the replot affords a competitive inhibition constant of 1.5×10^{-8} M. The data are indicative of linear competitive inhibition.

The low value of α, comparable to that seen for inhibition of AchE, was indicative of a strongly noncompetitive mode of inhibition of BuchE.

Kinetics of reversible noncovalent inhibition of THA were compared with those observed for NMA, an acridinium molecule structurally related to THA. NMA has been reported to cause linear mixed inhibition of AchE ($\alpha = 1.9$, $K_I = 4.6 \times 10^{-8}$ M) (19). With respect to BuchE, NMA caused linear mixed inhibition of $BuSch^+$ hydrolysis ($\alpha = 1.2$, $K_I = 2.6 \times 10^{-7}$ M).

Equilibrium association of THA with AchE and BuchE. Topographic specificity of THA was examined with respect to its capacity for association with AchE at either the peripheral anionic site or the active center. Propidium was used as a selective probe for the peripheral anionic site (12). Titration of AchE with propidium in the absence of THA afforded an equilibrium binding profile with a dissociation constant of 4.7×10^{-6} M (Fig. 5), in reasonable agreement with previously published values. In the presence of THA at a concentration of 8.5×10^{-6} M, 1250–2237 times its inhibition constant, propidium association displayed a saturable binding isotherm compatible with ligand association at a single class of homogeneous sites. From a Scatchard plot of the same data, the dissociation constant was calculated to be $7.7 \pm 0.7 \times 10^{-8}$ M, within 2-fold of that in the absence of THA (Fig. 5).

Decidium, containing an n-alkyl trimethylammonium moiety, was used for its selectivity at the active center of AchE (13–15). THA caused dissociation of >90% of the bound decidium. The dissociation profile was characterized by a slope of 0.95 ± 0.02, consistent with a competitive interaction (Fig. 6). The dissociation constant for THA, based on a K_D of 2.1×10^{-8} M for decidium, was calculated to be $7.0 \pm 0.4 \times 10^{-9}$ M, a value in close agreement with the inhibition constant.

The trimethylammonium moiety of decidium associates at the active center of BuchE. Association is accompanied by an increase in fluorescence at 615 nm (corrected), follows a saturable binding isotherm, and is characterized by a dissociation constant of $1.3 \pm 0.1 \times 10^{-7}$ M.[1] Titration of BuchE with THA caused dissociation of >90% of the bound decidium. The titration profile was characterized by a slope of 1.00 ± 0.03 (Fig. 6), consistent with a competitive interaction. The dissociation constant for THA, based on a K_D of 1.3×10^{-7} M for decidium,

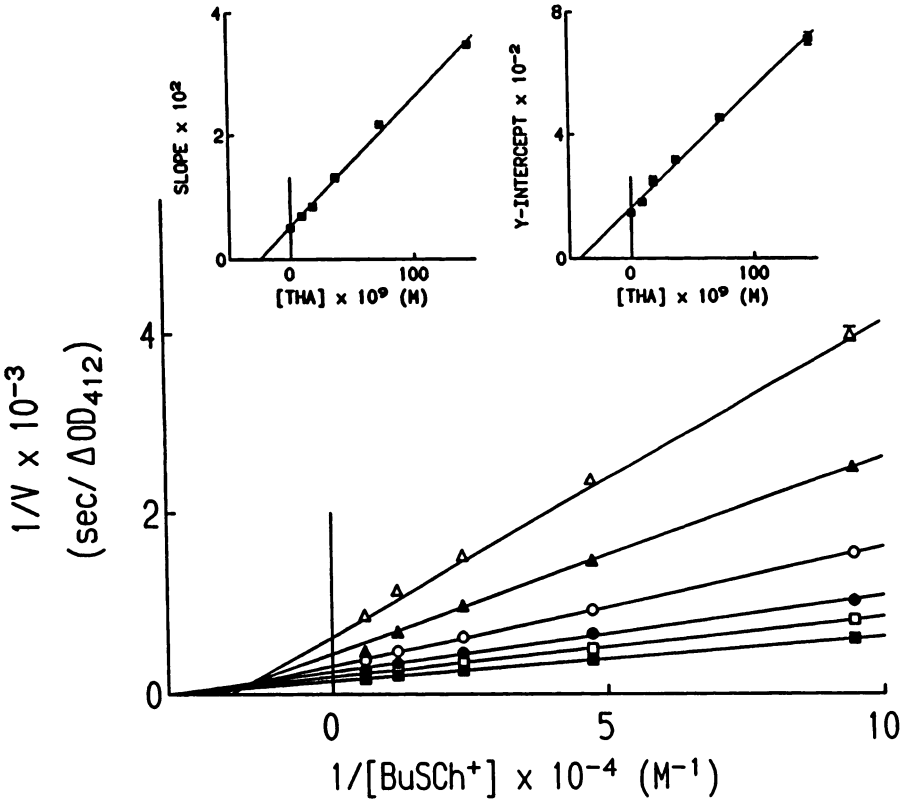

Fig. 4. Double-reciprocal plots for inhibition by THA of BuchE hydrolysis of $BuSch^+$. The enzyme was present at a concentration of 1.1×10^{-9} M, in a reaction medium of 0.01 M sodium phosphate buffer, pH 7.0, containing 0.2 M NaCl. ■, No THA; □, 9.23 nM; ●, 18.4 nM; ○, 36.8 nM; ▲, 73.4 nM; △, 146 nM. The value for k_{cat}, taken from the reciprocal of the y-intercept, was calculated to be 2.8×10^4 min^{-1}. The value for K_S, taken from the reciprocal of the x-intercept, was calculated to be 3.4×10^{-5} M. *Upper left inset*, replot of the reciprocal plot slopes versus THA concentration; the inhibition constant taken from the [*I*]-intercept was calculated to be 2.5×10^{-8} M. *Upper right inset*, y-intercept replot, from which α was determined to be 1.7. The data are indicative of linear mixed inhibition.

MOL PHARM
MOLECULAR PHARMACOLOGY
aspet
Downloaded from molpharm.aspetjournals.org at Universidade do Estado do Rio de Janeiro on December 4, 2012

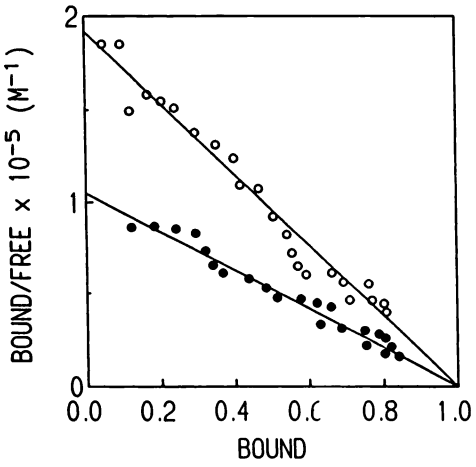

Fig. 5. Scatchard plots describing association of propidiam with AchE in the absence and presence of THA. Propidium association with AchE, present at a subunit concentration of approximately 3×10^{-6} M, was monitored directly by measuring fluorescence at 610 nm, upon excitation at 535 nm. In the absence of THA (○), propidium binding was characterized by a dissociation constant of 5.1×10^{-6} M. Averaged over two separate titrations, the dissociation constant was determined to be 4.7×10^{-6} M, in good agreement with the published value (12). When THA was present at a concentration of 8.5×10^{-6} M (●), propidium association was characterized by a dissociation constant of 9.7×10^{-6} M. Averaged over four separate titrations, the dissociation constant was determined to be $7.7 \pm 0.7 \times 10^{-6}$ M.

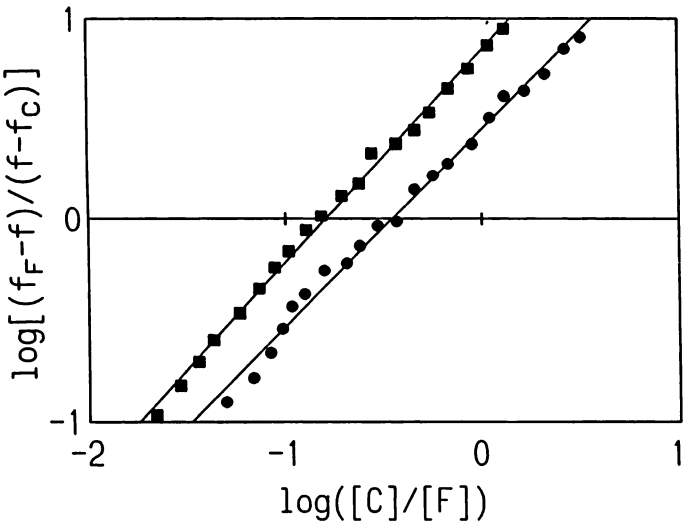

Fig. 6. Competitive dissociation by THA of decidium complexes with AchE and BuchE. This figure presents logarithmic analysis of THA dissociation of decidium complexes with AchE (●) and BuchE (■). Decidium was present at concentrations 20 times its dissociation constant and at least 2-fold greater than the enzyme concentration, as described in Experimental Procedures. For dissociation of decidium complexes of AchE, the slope was determined to be 0.95 ± 0.02. From the *x*-intercept of −0.489 and the known dissociation constant for decidium (2.1×10^{-8} M), the competitive dissociation constant for THA was calculated to be 6.8×10^{-9} M. Averaged over four separate determinations, the dissociation constant for THA was determined to be $7.0 \pm 0.4 \times 10^{-9}$ M. With respect to THA dissociation of decidium complexes with BuchE, the slope was determined to be 1.00 ± 0.03. From the *x*-intercept of −0.795 and the known dissociation constant for decidium (1.3×10^{-7} M), the competitive dissociation constant for THA with respect to association with BuchE was calculated to be 2.0×10^{-9} M. Averaged over four separate determinations, the dissociation constant for THA and BuchE was determined to be $1.9 \pm 0.1 \times 10^{-8}$ M.

was calculated to be $1.9 \pm 0.1 \times 10^{-8}$ M, a value in close agreement with the inhibition constant.

Discussion

Kinetic examination of THA association with AchE affords inhibition constants of 3.8×10^{-9} M with respect to hydrolysis of $AcSch^+$, 6.8×10^{-9} M with respect to 7AMC hydrolysis, and 1.5×10^{-8} M with respect to hydrolysis of M7C, values in close accord with those derived through competitive dissociation of decidium ($7.0 \pm 0.4 \times 10^{-9}$ M). With respect to BuchE, inhibition of $BuSch^+$ hydrolysis occurred at concentrations ($K_I = 2.5 \times 10^{-8}$ M) compatible with the dissociation constant derived through competitive dissociation of decidium ($K_D = 1.9 \pm 0.1 \times 10^{-8}$ M). For both enzymes, the linear mixed inhibition by THA of $AcSch^+$ and $BuSch^+$ hydrolysis reflects the presence of both competitive and noncompetitive components, whereas the low value of α indicates that the inhibition is essentially noncompetitive. Such inhibition might arise through ligand association at a site remote from the active center. The catalytic subunit of AchE contains a peripheral anionic site that, while topographically distinct from the active center, exerts allosteric control over enzyme hydrolysis. The peripheral site, therefore, represents one locus through which noncompetitive inhibition can occur. In an alternative mechanism, noncompetitive inhibition can arise through ligand association with a kinetic intermediate that appears during hydrolysis. Catalysis by AchE is known to engender formation of acyl intermediates that can associate with cationic inhibitors, representing another possible route to noncompetitive inhibition. Four lines of evidence, encompassing both kinetic and equilibrium criteria, support the latter mechanism.

First, the unit slope characterizing THA dissociation of decidium is compatible with a simple competitive relationship between THA and decidium. Because decidium associates with the trimethylammonium moiety at the active center of AchE, the competitive relationship with THA is compatible with active center association. Second, THA, present at concentrations >1250 times its inhibition constant, does not markedly alter propidium association. For mutually exclusive association of propidium and THA, the dissociation constant for propidium is predicted to be $(1 + [I]/K_I)$-fold, or more than 1251-fold greater than that observed in the absence of THA. Because the binding profiles for propidium in the presence and absence of THA fall within 2-fold of each other, the results demonstrate clearly that association of THA and propidium with AchE is not mutually exclusive.

Third, as indicated in scheme I, linear inhibition signifies that the reaction velocity can be driven to zero by sufficiently high inhibitor concentrations. The linear inhibition observed for THA indicates that the ternary complex (ESI) formed between enzyme, substrate, and THA is inactive. Nonlinear inhibition of hydrolysis, as observed upon peripheral site ligand inhibition by uncharged substrates such as 7AMC, signifies that high concentrations of inhibitor do not drive the reaction velocity to zero (19). This case is apparent by curvature in the slope and *y*-intercept replots and is obtained when $\beta > 0$, indicating that both ES and ESI remain productive and continue to undergo covalent reaction. Nonlinear inhibition represents a distinguishing feature of peripheral site occupation on covalent reactivity of AchE, in that peripheral site occupation blocks acylation by cationic but not uncharged acetyl ester

MOL PHARM
MOLECULAR PHARMACOLOGY
aspet
Downloaded from molpharm.aspetjournals.org at Universidade do Estado do Rio de Janeiro on December 4, 2012

substrates. Because ligands selective for the peripheral anionic site display nonlinear inhibition of uncharged substrates, the observation of linear inhibition of 7AMC by THA is inconsistent with peripheral site occupation.

Finally, noncompetitive inhibition can arise through a mechanism in which a cascade of kinetic intermediates is formed during hydrolysis of acetyl esters (scheme II). In this mechanism, as described by Krupka and Laidler (23), the enzyme-substrate complex (ES) undergoes covalent reaction to form a transient acyl intermediate (ES′), which reacts with water to form acetate and free enzyme. The rate constants k_2 and k_3 denote the rates of acylation and deacylation, respectively. Apparent noncompetitive inhibition can arise when I binds with a reaction intermediate, such as the acyl intermediate, ES′, and alters the velocity of the rate-determining step.

$$E + S \overset{K_S}{\rightleftharpoons} ES \xrightarrow{k_2} ES' \xrightarrow{k_3} E + P$$

SCHEME II

For $AcSch^+$, $k_3 \leq k_2$, and the rate-limiting step is deacylation (24). In this case, the essentially noncompetitive inhibition of $AcSch^+$ by THA can be attributed to inhibitor association with the acetyl-enzyme, ES′. For 7AMC, in contrast, $k_2 < k_3$, and the rate-limiting step is acylation (19). The observation of competitive inhibition of 7AMC hydrolysis is consistent with $k_2 < k_3$, with the consequence that inhibitor association with the acetyl-enzyme, because it occurs after the rate-determining step, is kinetically silent. The competitive inhibition of M7C hydrolysis by THA substantiates the mutually exclusive interaction between substrate and ligand. For hydrolysis of M7C, decarbamylation is slow, in comparison with the rate of carbamylation, and the pattern of inhibition reflects the initial interaction of E and I during the acyl-transfer step before formation of the covalent carbamyl-enzyme intermediate. Noncompetitive inhibition of AchE hydrolysis of $AcSch^+$, taken with the competitive inhibition of 7AMC and M7C hydrolysis, implicates mutually exclusive interactions between E and I and S and, therefore, direct interaction between THA and substrate at the active center. The net effect of THA association on hydrolysis of $AcSch^+$ is the slowing of deacylation, k_3. The slowing of deacylation during hydrolysis of 7AMC is not observed, because THA association is apparent only during the initial substrate-binding step.

Taken together, the kinetic and equilibrium indices uniformly indicate that THA associates at the active center of AchE and that the noncompetitive component of inhibition reflects ligand association with kinetic intermediates rather than association at the peripheral anionic site. This conclusion is in accord with intuition derived from structure-activity relationships. THA is structurally related to NMA, a well studied active center-selective cation (25, 26). It is of interest that the affinities of AchE and BuchE for THA are 10-fold higher than those for association with NMA. Whereas NMA possesses a hard cationic charge that is independent of the ionic milieu, THA possesses two potential proton-accepting moieties. THA likely exists with protonation at the more basic endocyclic nitrogen moiety. NMA shares with THA the capacity to block irreversible inactivation of AchE by organophosphorus agents (19, 22). Therefore, THA, as concluded for NMA, likely binds in close proximity to the nucleophilic residue, Ser-200. Kinetics of irreversible inhibition of an extended series of structurally related methylphosphonothioates indicate that the active center contains, in addition to an anionic site, an additional region that accommodates hydrophobic alkyl moieties (27). In this respect, it is not unreasonable that THA and NMA association proximal to Ser-200 can occur through association either within the anionic site or within the *n*-alkyl binding region. Although the data do not distinguish between these possibilities, it is noteworthy that aromatic ligands behave differently than *n*-alkyl bis- and monoquaternary cations in their blockade of irreversible inhibition by organophosphonates and their association at physically distinct regions within the active center (13, 19).

BuchE from human plasma and AchE from *Torpedo* show considerable amino acid sequence homology that includes the active center region containing the nucleophilic serine residue (28–30). Decidium association with BuchE appears to occur within the catalytic center of BuchE, compatible with the presence of an anionic site. The mutually exclusive relationship between association of THA and decidium is suggestive of an active center locus for THA association with BuchE. As seen through examination of point mutations of cDNA sequences of BuchE from brain neuroblastomas and glioblastomas (31), the presence of a distinct residue, Asp-70, appears to be important in promoting cation association of active center-selective ligands. The remarkable similarity in behavior of BuchE and AchE with respect to ligand association and the capacity for noncompetitive inhibition suggests operation of similar kinetic mechanisms underlying hydrolysis of acyl choline esters.

Finally, AchE appears in muscle and neuron as physically distinct molecular forms characterized as either globular or asymmetric species (32, 33). Examination of brain tissue from Alzheimer's patients reveals measurable reductions in the globular, largely intracellular, forms of AchE, and increases of >300% in the asymmetric species (3), a family of elongated, collagen-tailed forms destined for secretion into the extracellular matrix. Although the overall amounts of AchE appear to undergo reduction, it is of interest that the increased amounts of AchE occur among distinct species that, by virtue of their extracellular localization, are thought to subserve hydrolysis of Ach^+. The rationale underlying utilization of THA in treatment of Alzheimer's disease is based on the intuition that inhibition of AchE results in reduced rates of removal of Ach^+ from the synaptic cleft, thereby increasing the probability for effective encounter between neurotransmitter and the reduced numbers of muscarinic receptors. The high affinity characterizing association of THA and AchE might be anticipated to promote selective inhibition of the increased amounts of extracellular AchE. Such selectivity would be of particular importance in view of emerging evidence that concentrations of THA (>1 μM) substantially greater than those required for inhibition of AchE exhibit a multiplicity of activities, including blockade of K^+ channels (34–36), muscarinic receptors (37, 38), and high affinity choline uptake (39).

References

1. Katzman, R. Alzheimer's disease. *N. Engl. J. Med.* **314**:964–973 (1986).
2. Katzman, R., and T. Saitoh. Advances in Alzheimer's disease. *FASEB J.* **5**:278–286 (1991).
3. Younkin, S. G., B. Goodridge, J. Katz, G. Lockett, D. Nafziger, M. F. Usiak, and L. H. Younkin. Molecular forms of acetylcholinesterases in Alzheimer's disease. *Fed. Proc.* **45**:2982–2988 (1986).

MOL PHARM
MOLECULAR PHARMACOLOGY
aspet
Downloaded from molpharm.aspetjournals.org at Universidade do Estado do Rio de Janeiro on December 4, 2012

4. Fishman, E. B., G. C. Siek, R. D. MacCallum, E. D. Bird, L. Volicer, and J. K. Marquis. Distribution of the molecular forms of acetylcholinesterase in human brain: alterations in dementia of the Alzheimer type. *Ann. Neurol.* **19**:246–252 (1986).
5. Siek, G. C., L. S. Katz, E. B. Fishman, T. S. Korosi, and J. K. Marquis. Molecular forms of acetyl cholinesterase in subcortical areas of normal and Alzheimer disease brain. *Biol. Psychiatry* **27**:573–580 (1990).
6. Thal, L. J., P. A. Fuld, D. M. Masur, and N. S. Sharpless. Oral physostigmine and lecithin improve memory in Alzheimer disease. *Ann. Neurol.* **13**:491–496 (1983).
7. Summers, W. K., L. V. Majovski, G. M. Marsh, K. Tachiki, and A. Kling. Oral tetrahydroaminoacridine in long-term treatment of senile dementia, Alzheimer type. *N. Engl. J. Med.* **315**:1241–1245 (1986).
8. Relman, A. S. Special report: tacrine as a treatment for Alzheimer's dementia. *N. Engl. J. Med.* **324**:349–352 (1991).
9. Molloy, D. W., G. H. Guyatt, D. B. Wilson, R. Duke, L. Rees, and J. Singer. Effect of tetrahydroaminoacridine on cognition, function, and behavior in Alzheimer's disease. *Can. Med. Assoc. J.* **144**:29–34 (1991).
10. Heilbronn, E. Inhibition of cholinesterases by tetrahydroaminoacridine. *Acta Chem. Scand.* **15**:1386–1390 (1961).
11. Patocka, J., J. Bajgar, J. Bielavsky, and J. Fusek. Kinetics of inhibition of cholinesterases by 1,2,3,4-tetrahydro-9-aminoacridine *in vitro*. *Collect. Czech. Chem. Commun.* **41**:816–824 (1976).
12. Taylor, P., and S. Lappi. Interaction of fluorescence probes with acetylcholinesterase: the site and specificity of propidium binding. *Biochemistry* **14**:1989–1997 (1975).
13. Berman, H. A., and M. M. Decker. Kinetic, equilibrium, and spectroscopic studies on cation association at the active center of acetylcholinesterase: topographic distinction between trimethyl and trimethylammonium sites. *Biochim. Biophys. Acta* **872**:126–133 (1986).
14. Berman, H. A., and M. M. Decker. Kinetic, equilibrium and spectroscopic studies on dealkylation ("aging") of alkyl organophosphonyl-acetylcholinesterase: electrostatic control of enzyme topography. *J. Biol. Chem.* **261**:10646–10652 (1986).
15. Berman, H. A., M. M. Decker, M. W. Nowak, K. J. Leonard, M. McCauley, W. M. Baker, and P. Taylor. Site selectivity of fluorescent bisquaternary phenanthridinium ligands for acetylcholinesterase. *Mol. Pharmacol.* **31**:610–616 (1987).
16. Taylor, P., J. W. Jones, and N. M. Jacobs. Acetylcholinesterase from *Torpedo*: characterization of an enzyme species isolated by lytic procedures. *Mol. Pharmacol.* **10**:78–92 (1974).
17. Lockridge, O., and B. N. La Du. Loss of interchain disulfide peptide and dissociation of the tetramer following limited proteolysis of native human serum cholinesterase. *J. Biol. Chem.* **257**:12012–12018 (1982).
18. Ralston, J. S., A. R. Main, B. F. Kilpatrick, and A. L. Chasson. Use of procainamide gels in the purification of human and horse serum cholinesterases. *Biochem. J.* **211**:243–250 (1983).
19. Berman, H. A., and K. Leonard. Ligand exclusion on acetylcholinesterase. *Biochemistry* **29**:10640–10649 (1990).
20. Ellman, G. L., K.-D. Courtney, V. Andres, Jr., and R. M. Featherstone. A new and rapid calorimetric determination of acetylcholinesterase activity. *Biochem. Pharmacol.* **7**:88–95 (1961).
21. Riddles, P. W., R. L. Blakely, and B. Zerner. Ellman's reagent, 5,5′-dithiobis(2-nitrobenzoic acid): a reexamination. *Anal. Biochem.* **94**:75–81 (1979).
22. Wu, C. S., and J. T. Yang. Tacrine protection of acetylcholinesterase from inactivation by diisopropylfluorophosphate: a circular dichroism study. *Mol. Pharmacol.* **35**:85–92 (1989).
23. Krupka, R. M., and K. J. Laidler. Molecular mechanisms for hydrolytic enzyme action. I. Apparent noncompetitive enzyme inhibition, with special reference to acetylcholinesterase. *J. Am. Chem. Soc.* **83**:1445–1447 (1961).
24. Quinn, D. M. Acetylcholinesterase: enzyme structure, reaction dynamics, and virtual transition states. *Chem. Rev.* **87**:955–979 (1987).
25. Nolte, H.-J., T. L. Rosenberry, and E. Neumann. Effective charge on acetylcholinesterase sites determined from the ionic strength dependence of association rate constants with cationic ligands. *Biochemistry* **19**:3705–3711 (1980).
26. Mooser, G., and D. S. Sigman. Ligand binding properties of acetylcholinesterase determined with fluorescent probes. *Biochemistry* **13**:2299–2307 (1974).
27. Berman, H. A., and K. Leonard. Chiral reactions of acetylcholinesterase probed with enantiomeric methylphosphonothioates: noncovalent determinants of enzyme chiral preference. *J. Biol. Chem.* **264**:3942–3950 (1989).
28. Lockridge, O., C. F. Bartels, T. A. Vaughan, C. A. Wong, S. E. Norton, and L. L. Johnson. Complete amino acid sequence of human serum cholinesterase. *J. Biol. Chem.* **262**:549–557 (1987).
29. Arpagaus, M., A. Chatonnet, P. Masson, M. Newton, T. A. Vaughan, C. F. Bartels, C. P. Nogueira, B. N. La Du, and O. Lockridge. Use of polymerase chain reaction for homology probing of butyrylcholinesterase from several vertebrates. *J. Biol. Chem.* **266**:6966–6974 (1991).
30. Taylor, P. The cholinesterases. *J. Biol. Chem.* **266**:4025–4028 (1991).
31. Neville, L. F., A. Gnatt, R. Padan, S. Seidman, and H. Soreq. Anionic site interactions in human butyrylcholinesterase disrupted by two single point mutations. *J. Biol. Chem.* **265**:20735–20738 (1990).
32. Rotundo, R. L. Biogenesis and regulation of acetylcholinesterase, in *The Vertebrate Neuromuscular Junction* (M. M. Salpeter, ed.). Alan R. Liss, Inc., New York, 247–284 (1987).
33. Toutant, J. P., and J. Massoulie. Cholinesterase: tissue and cellular distribution of molecular forms and their physiological regulation, in *The Cholinergic Synapse* (V. P. Whittaker, ed.). Springer-Verlag, New York, 225–265 (1988).
34. Osterrieder, W. 9-Amino-1,2,3,4-tetrahydroacridine (THA) is a potent blocker of cardiac potassium channels. *Br. J. Pharmacol.* **92**:521–525 (1987).
35. Halliwell, J. V., and E. A. Grove. 9-Amino-1,2,3,4-tetrahydroacridine (THA) blocks agonist-induced potassium conductance in rat hippocampal neurones. *Eur. J. Pharmacol.* **163**:369–372 (1989).
36. Kotake, H., I. Hisatome, S. Matsuoka, H. Miyakoda, J. Hasegawa, and H. Mashiba. Inhibitory effect of 9-amino-1,2,3,4-tetrahydroacridine (THA) on the potassium current of rabbit sinoatrial node. *Cardiovasc. Res.* **24**:42–46 (1990).
37. Flynn, D. D., and D. C. Mash. Multiple *in vitro* interactions with and differential *in vivo* regulation of muscarinic receptor subtypes by tetrahydroaminoacridine. *J. Pharmacol. Exp. Ther.* **250**:573–581 (1989).
38. Hunter, A. J., T. K. Murray, J. A. Jones, A. J. Cross, and A. R. Green. The cholinergic pharmacology of tetrahydroaminoacridine *in vivo* and *in vitro*. *Br. J. Pharmacol.* **98**:79–86 (1989).
39. Buyukuysal, R. L., and R. J. Wurtman. Tetrahydroaminoacridine but not 4-aminopyridine inhibits high-affinity choline uptake in striatal and hippocampal synaptosomes. *Brain Res.* **482**:371–375 (1989).

Send reprint requests to: Harvey Alan Berman, Department of Biochemical Pharmacology, State University of New York at Buffalo, Buffalo, NY 14260.

MOL PHARM
MOLECULAR PHARMACOLOGY
aspet
Downloaded from molpharm.aspetjournals.org at Universidade do Estado do Rio de Janeiro on December 4, 2012